

Accepted for publication in the Astrophysical Journal

# A New Analysis of the O VI Emitting Nebula around KPD 0005+5106<sup>1</sup>

Ravi Sankrit<sup>2</sup>

*SOFIA Science Center/USRA, NASA Ames Research Center, Mail Stop 211-3, Moffett  
Field, CA 94035*

rsankrit@sofia.usra.edu

and

W. Van Dyke Dixon

*Department of Physics and Astronomy, Johns Hopkins University, 3400 N. Charles Street,  
Baltimore, MD 21218*

wvd@pha.jhu.edu

## ABSTRACT

We present observations of O VI  $\lambda 1032$  emission around the helium white dwarf KPD 0005+5106 obtained with the *Far Ultraviolet Spectroscopic Explorer*. Previously published data, reprocessed with an updated version of the calibration pipeline, are included along with new observations. The recent upward revision of the white dwarf's effective temperature to 200,000 K has motivated us to re-analyze all the data. We compare observations with photoionization models and find that the density of the O VI nebula is about  $10 \text{ cm}^{-3}$ , and that the stellar flux must be attenuated by about 90% by the time it impinges on the inner face of the nebula. We infer that this attenuation is due to circumstellar material ejected by KPD 0005+5106 earlier in its evolution.

*Subject headings:* circumstellar matter — planetary nebulae: general — stars: individual (KPD 0005+5106) — ultraviolet: ISM — white dwarfs

---

<sup>1</sup>Based on observations made with the NASA-CNES-CSA *Far Ultraviolet Spectroscopic Explorer*. *FUSE* is operated for NASA by the Johns Hopkins University under NASA contract NAS5-32985.

<sup>2</sup>Visiting Research Scientist, Johns Hopkins University, 3400 N. Charles Street, Baltimore, MD 21218

## 1. Introduction

The DO (helium-rich) white dwarf KPD 0005+5106 is the hottest known white dwarf star. Its effective temperature was measured to be 120,000 K by Werner et al. (1994), and recently revised upward to 200,000 K by Werner et al. (2007) based on the detection of Ne VIII lines in its spectrum. Subsequently, Werner et al. (2008a) identified emission from Ca X in its UV spectrum, the highest ionization stage of any element observed in a stellar photosphere. Weak X-ray emission at 1 keV detected with the *ROSAT* PSPC has been interpreted as evidence for a hot ( $\sim 2 \times 10^6$  K), fast, perhaps shock-heated wind, though it may be photospheric (O’Dwyer et al. 2003; Chu et al. 2004; Drake & Werner 2005; Werner et al. 2008b). Chu et al. (2004) find that the star is surrounded by an optical nebula, visible in [O III]  $\lambda 5007$  emission, roughly  $3^\circ$  in diameter. They find that the nebula contains about  $70 M_\odot$  of material, and argue that this large mass implies that the material must be interstellar rather than circumstellar. Closer in, Otte et al. (2004) discovered bright, diffuse O VI  $\lambda 1032$  emission extending at least  $3.5'$  from the star.

The Otte et al. (2004) study is based on data from 15 lines of sight observed with the *Far Ultraviolet Spectroscopic Explorer (FUSE)* between 2001 and 2003. KPD 0005+5106 was observed as a calibration target throughout the *FUSE* mission, and spectra of half a dozen additional sight lines are now available. Meanwhile, the *FUSE* data-reduction software has evolved considerably, particularly with the release of CalFUSE v3. The revised effective temperature of the white dwarf, the new data, and the improved calibration pipeline motivated us to re-examine the nature of the O VI emitting nebula around KPD 0005+5106.

## 2. Observations, Data Reduction, and Analysis

*FUSE* consists of four coaligned spectrographs. Two employ optics coated with Al+LiF and record spectra over the wavelength range 990–1187 Å; the other two use SiC coatings and are sensitive to wavelengths below the Lyman limit. The four channels overlap between 990 and 1070 Å. Each channel has three apertures that simultaneously sample different parts of the sky. The low resolution (LWRS) aperture is  $30'' \times 30''$  in size. The medium resolution (MDRS) aperture is  $4'' \times 20''$  and lies about  $3.5'$  from the LWRS aperture. The  $1.25'' \times 20''$  high-resolution (HIRS) aperture lies midway between the MDRS and LWRS apertures. A fourth location, the reference point (RFPT), is offset from the HIRS aperture by about  $1'$ . When a star is placed at the reference point, all three apertures sample the background sky. For a complete description of *FUSE*, see Moos et al. (2000) and Sahnou et al. (2000).

To identify observations for this study, we searched the Multimission Archive at Space

Telescope (MAST) for *FUSE* observations of KPD 0005+5106 obtained through the MDRS, HIRS, or RFPT apertures, for which the LWRS aperture should sample the background sky. Because its sensitivity at 1032 Å is more than twice that of any other channel, we consider only data from the LiF 1A channel. We use data obtained in time-tag mode, which preserves arrival time and pulse-height information for each photon event. Our final sample, consisting of data obtained along 21 lines of sight, is presented in Table 1; the location of each sight line is plotted in Figure 1. Our sight lines now range over more than 180° around the star.

The data were reduced using an implementation of CalFUSE v3.2, the final version of the *FUSE* data-reduction software package (Dixon et al. 2007), optimized for faint, diffuse emission. Details are given in Dixon et al. (2006), but we highlight a few points here: the program operates on one exposure at a time, producing a flux- and wavelength-calibrated spectrum from each. Background subtraction is turned off. Zero-point errors in the wavelength scale are corrected by fitting a synthetic emission feature to the Ly $\beta$  airglow line. The spectra from individual exposures are shifted to a heliocentric wavelength scale and combined. Finally, the spectra are binned by 14 pixels (53 km s<sup>-1</sup>), a value chosen so that two binned pixels just span a diffuse emission feature.

To improve the statistical significance of our results, we combine spectra with the lowest signal-to-noise ratios with those of adjacent sight lines, as noted in Table 2. The resulting spectra are fit with a synthetic O VI  $\lambda$ 1032 emission feature using the non-linear curve-fitting program SPECFIT (Kriss 1994). The model consists of a top-hat shaped function 106 km s<sup>-1</sup> in width, representing the LWRS aperture, convolved with a Gaussian, representing the instrument line-spread function ( $\sim$  25 km s<sup>-1</sup>) convolved with the intrinsic emission-line profile. Free parameters in the fit are the level and slope of the background (assumed linear) and the amplitude, central wavelength, and FWHM of the Gaussian.

Our model fits yield line intensities with  $I/\sigma(I) \geq 2.9$  for 14 spectra. The best-fit parameters are presented in Table 2. (Note that the sight lines are ordered anticlockwise, with those at radius 1.75' followed by those at radius 3.5'.) Measured intensities range from 7.3 to 22.1 kLU. (1 LU = 1 photon s<sup>-1</sup> cm<sup>-2</sup> sr<sup>-1</sup>.) A fit to the sum of all 14 spectra yields an intensity of  $15.5 \pm 0.8$  kLU, a line width of  $30 \pm 10$  km s<sup>-1</sup>, and a local standard of rest velocity  $v_{\text{LSR}} = 11 \pm 2$  km s<sup>-1</sup>. Individual lines of sight show considerable scatter about the mean velocity. Several sight lines have FWHM values  $< 25$  km s<sup>-1</sup>, indicating that their O VI features are unresolved. Two spectra show no evidence of O VI  $\lambda$ 1032 emission; for them, we compute  $3\sigma$  upper limits to the O VI intensity by first modeling the linear continuum, then increasing the strength of a model O VI  $\lambda$ 1032 line until  $\chi^2$  rises by 9 (corresponding to a  $3\sigma$  deviation for one interesting parameter; Avni 1976). Plots of selected spectra and best-fit models are presented in Figure 2. The asymmetric shapes of some model emission

features are artifacts of our sparse sampling of the model lines.

There are two caveats. First, these observations are relatively short. To maximize the signal-to-noise ratio of our spectra, we use all of the data, including that obtained during orbital day. To test for contamination by geocoronal emission (Shelton et al. 2007), we repeat the analysis, using only data obtained during orbital night. We find that, in all cases for which the night-only spectrum has significant exposure time ( $> 1500$  s), the day-plus-night and night-only line intensities agree within the night-only uncertainties. Second, we do not attempt to fit the fainter component of the O VI doublet at  $1038 \text{ \AA}$ . It is only half as bright as the  $1032 \text{ \AA}$  line (in an optically-thin medium) and may be blended with interstellar C II\*  $\lambda 1037$  or geocoronal O I  $\lambda 1039$ .

The reddening toward KPD 0005+5106,  $E(B - V) = 0.06$  (§3.1), reduces the observed O VI intensity by  $\sim 55\%$  (Fitzpatrick 1999). The line intensities presented in Figure 1 and Table 2 are not corrected for this extinction. The stellar spectrum shows strong absorption from molecular hydrogen (Murphy et al. 2004). The  $\text{H}_2$  absorption feature most likely to overlap the O VI  $\lambda 1032$  emission line is the Lyman (6,0)  $R(4)$  transition at  $1032.35 \text{ \AA}$ . Its velocity,  $v_{\text{LSR}} = -13 \text{ km s}^{-1}$  (J. Kruk, private communication), places it some  $100 \text{ km s}^{-1}$  from the velocity of the summed O VI emission features derived above. Assuming that both the O VI emitting and  $\text{H}_2$  absorbing gas are photoexcited and have low turbulent velocities, then their intrinsic line widths should be about  $10 \text{ km s}^{-1}$  (a value consistent with the  $30 \text{ km s}^{-1}$  width of the summed O VI feature, which includes the instrumental line spread function). The O VI emission and  $\text{H}_2$  absorption features are thus well separated.

Our results generally agree with those of Otte et al. (2004). Where they differ, our intensities tend to be lower. Examples are sight lines S4044403 and M1070224 (map keys S43 and M24), which Otte et al. fit separately, obtaining intensities of  $25 \pm 4$  and  $25 \pm 7$  kLU, respectively. Because the intensity of the M24 feature is poorly constrained in our fits, we combine the two spectra and obtain a best-fit intensity of  $17.0 \pm 2.5$  kLU. For sight line M1070223, the difference is more extreme: our intensity of  $9.4 \pm 3.0$  kLU is half of the  $18 \pm 8$  kLU reported by Otte et al., though their value is poorly constrained. Note that, for most lines of sight, Otte et al. use only data from the nighttime portion of the orbit.

### 3. Modeling the Nebular Emission

A star with an effective temperature of  $200,000 \text{ K}$  is expected to produce a significant amount of high energy radiation, capable of ionizing oxygen up to  $\text{O}^{5+}$ . Thus, the O VI emission we detect around KPD 0005+5106 is most likely from gas photoionized by the

star. We explore the conditions in the nebula by running photoionization models. The calculations, described in detail in §3.2, were performed with version 08.00 of Cloudy, last described by Ferland et al. (1998).

We require the models to reproduce two observational results: the “typical” O VI intensity and the spatial extent of the [O III] emission detected by Chu et al. (2004). As we will show, these conditions place strong constraints on the incident flux and on the density of the emitting gas. We do not seek to explain the distribution of the O VI emission, nor the variations in its intensity (Figure 1), using these model calculations. First, we discuss the stellar parameters of KPD 0005+5106, including its distance. The latter is necessary for obtaining the spatial scales of the emitting regions.

### 3.1. Stellar Parameters

In their initial analysis of KPD 0005+5106, Werner et al. (1994) derive an effective temperature  $T_{\text{eff}} = 120,000$  K and a surface gravity  $\log g = 7.0$ . Comparing these parameters with post-asymptotic giant branch (post-AGB) evolutionary tracks, they estimate the star’s mass to be  $M_* = 0.59 M_{\odot}$ . Comparing its V-band flux ( $V = 13.32$ ; Downes et al. 1985) with model predictions, they derive a distance to the star of 270 pc. At this distance, the 3.5’ radius of the outer set of *FUSE* sight lines (Figure 1) corresponds to a physical extent of 0.27 pc.

The detection of Ne VIII absorption features in the *FUSE* spectrum of KPD 0005+5106 requires an upward revision of its effective temperature. Werner et al. (2007) find that the Ne VIII lines are best fit by models with  $T_{\text{eff}} = 180,000 - 200,000$  K and  $\log g = 6.5 - 7.0$ . Subsequently, Ca X emission lines were identified in the *FUSE* spectrum, and fits to these lines yield  $T_{\text{eff}} = 200,000 - 220,000$  K and  $\log g = 6.2 - 6.5$  (Werner et al. 2008a). For both species, the best-fit value of the surface gravity rises with effective temperature. Werner et al. (2007) point out that the star’s He II lines, in both the UV and the optical, are better fit by a model with  $T_{\text{eff}} = 200,000$  K and  $\log g = 6.5$  than by the original  $T_{\text{eff}} = 120,000$  K,  $\log g = 7.0$  model.

K. Werner has kindly provided us with a synthetic spectrum of the star. It is based on a  $T_{\text{eff}} = 200,000$  K and  $\log g = 6.5$  model atmosphere composed of He, C, O and Ne, with C = 0.003, O = 0.0006, and Ne = 0.01 by mass (Werner et al. 2008a). J. Kruk has provided the fully-reduced *FUSE* spectrum of KPD 0005+5106. From these, we can estimate both the star’s interstellar reddening and its distance. We begin by scaling the synthetic spectrum according to the reddening law of Fitzpatrick (1999) for various values of the color excess

$E(B - V)$ . We scale the result to match the star’s V-band flux. Finally, we compare the predicted and observed flux at 1060 Å in the *FUSE* spectrum. We find that the *FUSE* data are best fit by  $E(B - V) = 0.06$ , a value similar to the  $E(B - V) = 0.07$  derived by Downes et al. (1985) from *IUE* data.

As Werner et al. (2008b) point out, an effective temperature  $T_{\text{eff}} = 200,000$  K and a surface gravity  $\log g = 6.5$  place KPD 0005+5106 on the  $0.7 M_{\odot}$  post-AGB evolutionary track of Wood & Faulkner (1986). Adopting this mass and surface gravity, we derive a radius  $R_{*} = 0.08 R_{\odot}$ . The scale factor required to make the reddened model (at 5500 Å) match the star’s V-band flux is  $\text{SF} = 1.4 \times 10^{-23}$ . Given the star’s radius and this scale factor, its distance is simply  $d^2 = \pi R_{*}^2 / \text{SF}$  (Kurucz 1979), or  $d = 820$  pc. At this distance, the  $1.75'$  radius of the inner set of *FUSE* sight lines corresponds to  $\sim 0.42$  pc ( $1.3 \times 10^{18}$  cm), the  $3.5'$  radius of the outer set corresponds to  $\sim 0.84$  pc ( $2.6 \times 10^{18}$  cm), and the  $1.5^{\circ}$  radius of the [O III] nebula corresponds to  $\sim 21$  pc ( $6.6 \times 10^{19}$  cm).

We repeat the calculations using a second synthetic spectrum (also provided by K. Werner) with  $T_{\text{eff}} = 180,000$  K and  $\log g = 6.5$ . Scaling the model to match the observed V-band and 1060Å fluxes, we derive a color excess  $E(B - V) = 0.06$ , which is the same as for the hotter model. Assuming the same stellar mass as before, we derive a distance to the star of 780 pc.

Small changes in the surface gravity affect the stellar radius, but do not significantly alter the overall shape of the emergent continuum. A star with  $T_{\text{eff}} = 200,000$  K and  $\log g = 6.2$  would have a radius of  $0.11 R_{\odot}$ , which is about 40% larger than that for  $\log g = 6.5$ . The luminosity would therefore be greater by about 90% (since  $L \propto R^2$ ), and the derived distance to the star would increase to 1.2 kpc.

### 3.2. Cloudy Models

Cloudy is a versatile code that can be used to calculate the ionization structure and emission from photoionized gas under a broad range of conditions. Our models for the O VI nebula detected by *FUSE* are relatively simple. We assume an ionization-bounded slab of uniform density illuminated by the white dwarf. The main input parameters are the shape of the ionizing continuum, the incident flux on the cloud surface, the density structure of the gas, and the elemental abundances in the gas. Calculations are performed in one dimension assuming spherical symmetry; however, the effective geometry can be made plane parallel by choosing a large radius of curvature.

In our models, the abundances of elements are held fixed. We use the default solar

values as specified in Cloudy: C and O from Allende Prieto et al. (2001, 2002); N, Ne, Mg, Si and Fe from Holweger (2001); and the rest from Grevesse & Sauval (1998). We take the  $T_{\text{eff}} = 200,000$  K synthetic spectrum of KPD 0005+5106 as the shape of the incident continuum. (In §3.2.2 we use the  $T_{\text{eff}} = 180,000$  K spectrum to study how the results depend on the effective temperature of the star.) The incident flux and the gas density are allowed to vary (§3.2.3).

The physical distance from the star to the nebula scales with the distance from the star to the earth. The stellar distance is derived by scaling the model spectrum to match the observed fluxes in the V-band and at  $1060 \text{ \AA}$ . Therefore the flux normalization at the nebula does not depend directly on the distance between us and the star, but rather on the stellar flux observed at earth and the angular separation between the star and the inner face of the nebula, which we take to be  $1.7'$ .

### 3.2.1. Initial model

We first explore the case of the unattenuated stellar continuum incident on the O VI emitting nebula. The inner face of the nebula is assumed to be  $1.7'$  from the star, placing it just within the inner set of *FUSE* observations (clearly it can be no further away). This corresponds to a distance of  $1.3 \times 10^{18}$  cm at 820 pc. The normalization of the continuum may be described in terms of the flux of photons with energy greater than or equal to 113.9 eV, which is the energy required to ionize  $\text{O}^{4+}$  to  $\text{O}^{5+}$ . (This ionization energy corresponds to a photon frequency of about  $2.76 \times 10^{16}$  Hz.) From the synthetic spectrum of KPD 0005+5106, we find that the luminosity of such high-energy photons is  $\sim 2.8 \times 10^{46}$  photons  $\text{s}^{-1}$ . The flux of these photons at the inner face of the nebula is  $\sim 1.4 \times 10^9$  photons  $\text{s}^{-1} \text{ cm}^{-2}$ . For this initial model, we choose a hydrogen number density of  $1 \text{ cm}^{-3}$ , which is a typical value for the interstellar medium (ISM).

The calculations predict that the O VI emitting zone extends about 20 kpc, and that the O VI  $\lambda 1032$  emissivity is about  $1.5 \times 10^{-24}$  erg  $\text{s}^{-1} \text{ cm}^{-3}$  over most of the region. O VI  $\lambda 1032$  is a resonance line, and the Cloudy predictions of emissivity take into account radiative transfer effects via the escape probability formalism. Although the escape probabilities are calculated for a one-dimensional slab, we assume that the predicted emissivity holds for our observed lines of sight, which lie perpendicular to the direction of the stellar flux vector through the model nebula. Furthermore, we assume that the path length through the nebula is about  $4.2 \times 10^{18}$  cm, which is roughly equal to the extent of the O VI emission in the plane of the sky (about  $5.7'$ , the distance between sight lines M08 and M23 in Figure 1). Using these values, we find that the expected intensity from the model nebula is  $\sim 5 \times 10^{-7}$  erg

$\text{s}^{-1} \text{cm}^{-2} \text{sr}^{-1}$ . A color excess  $E(B - V) = 0.06$  (§ 3.1) toward KPD 0005+5106 corresponds to an extinction at  $1032\text{\AA}$  of about a factor of 2 (Fitzpatrick 1999). Therefore, the model predicts that the observed intensity would be about  $2.5 \times 10^{-7} \text{erg s}^{-1} \text{cm}^{-2} \text{sr}^{-1}$ , which equals about 13,000 LU. This value is consistent with the *FUSE* observations.

Although this model reproduces the observed O VI intensity, it does not correctly reproduce the extent of the optical nebula. In the model, the [O III] emission arises beyond the O VI, at a distance of between 20 and 32 kpc from the star. This is about three orders of magnitude larger than the  $\sim 20$  pc radius of the [O III] nebula detected by Chu et al. (2004).

### 3.2.2. $T_{\text{eff}} = 180,000$ K model

The lower limit on the effective temperature of KPD 0005+5106 is 180,000 K. We calculate a model using the  $T_{\text{eff}} = 180,000$  K synthetic spectrum to examine the sensitivity of the nebular properties to the stellar effective temperature. All other model parameters remain unchanged from the initial model.

The luminosity of  $\text{O}^{4+}$  ionizing photons is  $\sim 1.4 \times 10^{46}$  photons  $\text{s}^{-1}$ , about half that of the 200,000 K stellar spectrum. Their flux is  $\sim 6.8 \times 10^8$  photons  $\text{s}^{-1} \text{cm}^{-2}$  at the inner face of the nebula.

The O VI zone extends about 12 kpc, just over half the distance predicted by the 200,000 K model. The total O VI flux from the 180,000 K model nebula is only half that of the 200,000 K model. However, the intensity in the inner few kpc is about 20% higher. This is because more of the  $\text{O}^{5+}$  ions are ionized to  $\text{O}^{6+}$  by the 200,000 K spectrum than the 180,000 K spectrum. The [O III] emission arises at a distance of between 12 and 22 kpc from the star. This is still almost three orders of magnitude larger than the observed radius of the optical nebula.

If the effective temperature of KPD 0005+5106 were at the lower limit allowed by the Ne VIII lines, the unattenuated flux impinging on gas at typical interstellar densities would still produce an optical nebula much larger than observed. If the temperature were at the higher limit (220,000 K), the discrepancy would be increased. In the rest of this paper, we consider only the best-fit 200,000 K synthetic spectrum for KPD 0005+5106.



### 3.2.3. Fiducial model

We ran a grid of models using the  $T_{\text{eff}} = 200,000$  K synthetic spectrum for the continuum shape, varying the incident flux level and the density of the emitting gas. The incident flux levels ranged from the unattenuated stellar continuum used in the initial model down to one-tenth this value. (The latter corresponds to  $1.4 \times 10^8$   $\text{O}^{4+}$  ionizing photons  $\text{s}^{-1} \text{cm}^{-2}$ .) The hydrogen number densities ranged from  $1 \text{cm}^{-3}$  to  $100 \text{cm}^{-3}$ .

For models in which the continuum is unattenuated, a gas density  $n_{\text{H}}$  of about  $40 \text{cm}^{-3}$  is required to produce an [O III] nebula with a radius of about 20 pc. In that case, however, the predicted O VI intensity is over 200 times the observed value. As the incident flux is lowered, the density required to reproduce the observed radius of the [O III] nebula also decreases. For each such combination, the predicted O VI intensity decreases with incident flux and density, matching the observed values only when the incident flux is  $\sim 10\%$  of the unattenuated value. The corresponding hydrogen density in the gas is  $10 \text{cm}^{-3}$ . We take this to be the fiducial model for the nebula around KPD 0005+5106.

In Figure 3 we plot the predicted emissivities of O VI, [O III], and  $\text{H}\alpha$  against depth into the cloud. The average O VI emissivity out to a few parsec is about  $2 \times 10^{-24} \text{erg s}^{-1} \text{cm}^{-3}$ . This emissivity is slightly higher than that predicted by the initial model and, under the same assumptions used above, yields an observed intensity of 17,300 LU. The O VI nebula would be visible out to a few parsecs, i.e. beyond the outer ring of *FUSE* observations. The [O III] emissivity falls rapidly beyond about 24 pc, and the  $\text{H}\alpha$  emissivity extends slightly beyond 26 pc. The total [O III] to  $\text{H}\alpha$  flux ratio is about 6. This is consistent with the conclusion of Chu et al. (2004) that the  $\text{H}\alpha$  nebulosity associated with the nebula around KPD 0005+5106 is faint compared with the [O III].

The presence of photoionized O VI emission around a hot white dwarf is not unexpected. As shown by our model calculations, a 200,000 K star can maintain oxygen in this highly ionized state out to a distance of several kiloparsecs for typical ISM gas densities and can produce the observed O VI  $\lambda 1032$  intensity. (A similar point was made by Panagia & Terzian 1984, who showed that UV radiation from hot white dwarfs can maintain the presence of  $\text{C}^{3+}$  in the Galactic halo.) The puzzling result is that, in order to produce the observed O VI emission and an [O III] emitting zone confined to a radius of  $\sim 20$  pc, the ionizing continuum must be attenuated by about 90% between its emergence from the stellar surface and its incidence on the inner face of the nebula. In the next section, we discuss how this attenuation may be explained by the presence of circumstellar material around the white dwarf.

## 4. Discussion

### 4.1. Circumstellar material around KPD 0005+5106

The prior evolution of KPD 0005+5106 – and in particular its mass-loss history – are unknown. However, the star is expected to be surrounded by material lost while it was on the asymptotic giant branch. We make the assumption that a shell of material surrounds the star and examine the effect of such a shell on the stellar continuum. To do so, we calculate Cloudy models with the KPD 0005+5106 ( $T_{\text{eff}} = 200,000$  K) spectrum impinging on a shell and compare the emergent continuum with the incident.

From the Wood & Faulkner (1986) evolutionary track, we estimate that KPD 0005+5106 left the asymptotic giant branch some 2000 years ago, after ejecting its outer envelope. We thus fix the inner radius of the shell to be  $1 \times 10^{17}$  cm, the distance traveled in 2000 years by material moving at a typical PN expansion velocity of  $20 \text{ km s}^{-1}$ . Assuming that envelope ejection took a few thousand years, we fix the outer radius of the shell at three times the inner radius. The density, assumed to be uniform, is treated as a variable parameter. Abundances are fixed at the solar values. We find that the continuum above 113.9 eV is attenuated by about 90% when the density of the gas in the shell is  $n_{\text{H}} = 3500 \text{ cm}^{-3}$ . The total mass in the shell (assuming that it covers  $4\pi$  steradians) is then  $\sim 0.4 M_{\odot}$ , comparable to the  $0.2 M_{\odot}$  typical of planetary nebulae.

The shape of the emergent spectrum differs from that of the KPD 0005+5106 synthetic spectrum in several ways. There is a sharp decrease at the He II edge at 54.4 eV from which the spectrum begins to recover at  $\sim 100$  eV. While the  $\text{O}^{4+}$  ionizing continuum is reduced by 90%, the continuum between 54.4 eV and 100 eV is reduced by over 99%. The continuum between 13.6 eV and 54.4 eV is reduced by only about 70%.

We next calculate a Cloudy model of the nebula using this emergent spectrum propagated out to the inner face of the nebula ( $1.3 \times 10^{18}$  cm from the star). As described above, the shell density is chosen such that the flux of  $\text{O}^{4+}$  ionizing photons incident on the nebula is the same as that for the fiducial model. The hydrogen density in the nebula is  $10 \text{ cm}^{-3}$ , also equal to that in the fiducial model. The difference in the shape of the continuum has an impact on the predicted properties of the photoionized nebula.

The resulting model has an O VI zone that extends out to only about 2 pc, which is much smaller than that predicted by the fiducial model (Figure 3), but still extends beyond the outer ring of *FUSE* observations (Figure 1). The O VI intensity in the inner 1 pc (which encompasses the *FUSE* sight lines), however, is about 3 times that of the fiducial model. The [O III] zone extends out to 45 pc, about twice that predicted by the fiducial model (and

thus about twice the observed extent of the optical nebula).

The O VI intensity and the extent of the [O III] zone can be brought closer to the observed values if the flux emergent from the shell is reduced by an additional 32%, such that there are  $\sim 9.5 \times 10^7$  O<sup>4+</sup> ionizing photons s<sup>-1</sup> cm<sup>-2</sup> impinging on the nebula. A model with this lower flux yields an O VI zone extending about 2 pc from the star (as above). The O VI intensity in the inner 1 pc is within 5% of that predicted by the fiducial model, and the [O III] zone extends out to about 28 pc.

The gas density in the shell, its inner and outer radii, and the abundances of elements are all unconstrained parameters of the models. Additionally, the nebular gas density may be adjusted. Because there are no independent observational constraints on the putative circumstellar shell around KPD 0005+5106, more detailed calculations are not warranted.

We have shown (in §3.2) that in order to explain the O VI and [O III] observations of the nebula around KPD 0005+5106, the stellar flux must be attenuated. We have shown that this attenuation can be achieved by a shell of gas with properties consistent with mass loss from the star while on the asymptotic giant branch. We have further shown that the emergent spectrum is capable of photoionizing a nebula and producing the observed O VI and [O III] emission. However, we do not make any attempt to model both the shell and the nebular emission self-consistently. A shell such as the one we have assumed would produce its own emission. To our knowledge, there has not been a careful examination of the region around the star at sufficiently high resolution to place strong limits on any such emission.

#### 4.2. Spatial distribution of the O VI emission

It is clear from Figure 1 that the O VI emission has an azimuthal structure, with the faintest emission from the southern and northwestern edges of our sample and the brightest towards the southwest. The pattern is as clearly seen in Table 2, where the intensities exhibit a monotonic increase followed by a monotonic decrease going around the inner and outer rings. The only exception is sight line M34. The M34 value may be less reliable than the others because it has the shortest exposure time and is barely a  $3\sigma$  detection. If we ignore M34, then all the sight lines outside of the cone between lines connecting the white dwarf and M09 on one side and M24 on the other have O VI intensities less than or equal to 9.5 kLU. Within this cone, all sight lines have O VI intensities greater than or equal to 14.5 kLU. At the edges of the cone, only the inner ring shows the brighter O VI; M08 and M23 are fainter (Figure 1).

The observed distribution of the O VI intensities could be due to an azimuthal depen-

dence of either (i) the gas density in the nebula or (ii) the incident ionizing flux. We examine the conditions necessary for each of these alternatives, restricting ourselves to the predictions from one-dimensional models with uniform gas density.

For a given incident flux, the ionization parameter (ratio of ionizing photon density to gas density) decreases with increasing density, while the emission measure increases with increasing density. Thus, there is some value of density at which the O VI emissivity peaks. Our fiducial model assumes a gas density of  $10 \text{ cm}^{-3}$ . Raising the density to  $15 \text{ cm}^{-3}$  reduces the O VI emissivity by a factor of 1.5. If the density is  $20 \text{ cm}^{-3}$ , then the emissivity falls by a factor of 2.2. These emissivities yield observed intensities (under the path length assumptions used in §3.2) of 11.5 kLU and 7.9 kLU, respectively. Higher-density models also predict smaller and brighter [O III] nebulae than the fiducial model does, but no obvious azimuthal structure is seen in the [O III] images presented by Chu et al. (2004). A model with a density of  $1 \text{ cm}^{-3}$  predicts an O VI emissivity that is half the value of the fiducial model, but is ruled out because its [O III] zone extends to 2 kpc.

If the gas density is fixed, then a lower incident flux will yield fainter O VI emission. An incident flux 90% that of the fiducial model results in a factor of 1.4 drop in the O VI intensity. If the incident flux is 80% that of the fiducial model, then the intensity drops by a factor of just over 2. These values correspond to observed intensities of 12.5 kLU and 8.5 kLU respectively. The [O III] intensity and the extent of the [O III] emitting region are not strongly affected by changes in the incident flux – they change by factors of less than 20% among these models.

Spatial variations in the flux incident upon the O VI emitting nebula could be achieved by moderate density variations in the circumstellar shell around KPD 0005+5106. For example, in the shell considered in §4.1, if the density were  $4000 \text{ cm}^{-3}$  rather than  $3500 \text{ cm}^{-3}$ , then the  $\text{O}^{4+}$  ionizing continuum would be attenuated by about 98%, rather than 90%. The circumstellar shell is not an opaque object casting a shadow, but a source of diffuse radiation, with considerable angular extent when viewed from any point on the inner face of the nebula. Therefore we cannot simply infer the azimuthal structure of this shell based on the observed distribution of O VI intensities. Calculating the radiative transfer through the circumstellar shell to derive the incident continuum at each point in the nebula is beyond the scope of this work.

Of the two alternatives for explaining the observed azimuthal distribution of O VI emission, the latter, i.e., ionizing flux variations, is the one that has less effect on the distribution of [O III] emission. Therefore, we suggest that it is the more straightforward explanation.

One implicit assumption in all of our models is that the O VI and [O III] arise in a

single nebula with uniform density. This need not be the case. The mass loss of stars on the asymptotic giant branch is a complex process; in the case of KPD 0005+5106, up to  $2 M_{\odot}$  may have been lost over a period of  $10^4 - 10^5$  years prior to the final mass ejection that resulted in the circumstellar shell we have inferred in §4.1. If such were the case, then it would be necessary to consider (at least) an outer region of circumstellar material and the interstellar medium as independent emitting regions. One may then naively expect that all the O VI arises in the former, while the [O III] emission is dominated by the latter. Without further data, detailed explorations of such a scenario are premature.

## 5. Concluding Remarks

In this paper, we have presented a new analysis of the O VI  $\lambda 1032$  emission around the hot helium-rich white dwarf KPD 0005+5106. At the time of our earlier analysis (Otte et al. 2004), the star was believed to have an effective temperature of 120,000 K and lie at a distance of 270 pc. Since then, the effective temperature of the star has been revised (Werner et al. 2007), and consequently its inferred distance has increased to 820 pc (§3.1).

We have modeled our O VI measurements and the [O III]  $\lambda 5007$  emission around the star (Chu et al. 2004) as a photoionized nebula. We have used a synthetic spectrum of KPD 0005+5106 for the ionizing continuum and treated the nebula itself as a uniform, one-dimensional slab. Based on the comparison of models with data, we have inferred the existence of a circumstellar shell between the star and the O VI emitting nebula that attenuates the stellar flux by about 90%. We find that the nebula has a density of  $\sim 10 \text{ cm}^{-3}$ .

The distribution of O VI intensities on the plane of the sky shows a clear azimuthal structure. This structure may be due to a variation either of the gas density or of the incident flux. Within the framework of our simple models, we present the conditions under which we may expect the observed O VI intensity distribution for each alternative. We find that variations in the density would affect the brightness and the extent of the [O III] nebula in ways that probably would be observable, but which are not seen. However, a more careful examination of the optical emission with accurate photometry is required before any definitive statement can be made. The O VI intensity is more sensitive to variations in the incident flux, and the observed differences can be explained without affecting the properties of the predicted [O III] emission.

Our results clearly highlight the need for a thorough examination of the region around KPD 0005+5106. One possible tracer of high ionization gas is [Ne V]  $\lambda 3426$ . Our Cloudy models predict that the strength of this line is about 10 times that of O VI  $\lambda 1032$ . A

photometric, narrowband imaging study of the nebula in [O III] and [Ne V] emission would yield diagnostic information about the distribution of material and the ionization structure of the nebula. We have inferred the existence of a circumstellar shell based on the synthetic spectrum of KPD 0005+5106 and photoionization models for the nebular emission. Its existence is plausible considering the evolutionary history of stars on the asymptotic giant branch. A direct observation of such a shell would be of great value.

The authors thank Birgit Otte for initiating this project and providing the software used to construct Figure 1, Klaus Werner for providing synthetic spectra used in their analysis of KPD 0005+5106, and Jeff Kruk for providing the star’s fully-reduced *FUSE* spectrum. We acknowledge with gratitude the extraordinary efforts of the *FUSE* operations team to make this mission successful. We thank the referee for comments that motivated an extension of our analysis and a clearer presentation of our results. This research has made use of the NASA Astrophysics Data System (ADS) and the Multimission Archive at the Space Telescope Science Institute (MAST). STScI is operated by the Association of Universities for Research in Astronomy, Inc., under NASA contract NAS5-26555. Support for MAST for non-HST data is provided by the NASA Office of Space Science via grant NAG5-7584 and by other grants and contracts. The curve-fitting program SPECFIT runs in the IRAF environment. The Image Reduction and Analysis Facility is distributed by the National Optical Astronomy Observatories, which is supported by the Association of Universities for Research in Astronomy (AURA), Inc., under cooperative agreement with the National Science Foundation. This work is supported by NASA grant NNX06AD30G to the Johns Hopkins University, and by the Universities Space Research Association.

*Facilities:* FUSE.

## REFERENCES

- Allende Prieto, C., Lambert, D. L., & Asplund, M. 2001, *ApJ*, 556, L63
- . 2002, *ApJ*, 573, L137
- Avni, Y. 1976, *ApJ*, 210, 642
- Chu, Y.-H., Gruendl, R. A., Williams, R. M., Gull, T. R., & Werner, K. 2004, *AJ*, 128, 2357
- Dixon, W. V., Sankrit, R., & Otte, B. 2006, *ApJ*, 647, 328
- Dixon, W. V. et al. 2007, *PASP*, 119, 527
- Downes, R. A., Liebert, J., & Margon, B. 1985, *ApJ*, 290, 321
- Drake, J. J. & Werner, K. 2005, *ApJ*, 625, 973
- Ferland, G. J., Korista, K. T., Verner, D. A., Ferguson, J. W., Kingdon, J. B., & Verner, E. M. 1998, *PASP*, 110, 761
- Fitzpatrick, E. L. 1999, *PASP*, 111, 63
- Grevesse, N., & Sauval, A. J. 1998, *Space Science Review*, 85, 161
- Holweger, H. 2001, Joint SOHO/ACE Workshop “Solar and Galactic Composition”, 598, 23
- Kriss, G. A. 1994, in *ASP Conf. Ser. 61, Astronomical Data Analysis Software and Systems III*, ed. D. R. Crabtree, R. J. Hanisch, & J. Barnes (San Francisco: ASP), 437
- Kurucz, R. L. 1979, *ApJS*, 40, 1
- Moos, H. W. et al. 2000, *ApJ*, 538, L1
- Murphy, K. D., Williger, G. M., & Kruk, J. W. 2004, *BAAS*, 36, 1436
- O’Dwyer, I. J., Chu, Y.-H., Gruendl, R. A., Guerrero, M. A., & Webbink, R. F. 2003, *AJ*, 125, 2239
- Otte, B., Dixon, W. V., & Sankrit, R. 2004, *ApJ*, 606, L143
- Panagia, N., & Terzian, Y. 1984, *ApJ*, 287, 315
- Sahnow, D. J. et al. 2000, *ApJ*, 538, L7
- Shelton, R. L., Sallmen, S. M., & Jenkins, E. B. 2007, *ApJ*, 659, 365

Werner, K., Heber, U., & Fleming, T. 1994, *A&A*, 284, 907

Werner, K., Rauch, T., & Kruk, J. W. 2007, *A&A*, 474, 591

—. 2008a, *A&A*, 492, L43

—. 2008b, in *Astronomical Society of the Pacific Conference Series*, Vol. 391, *Hydrogen-Deficient Stars*, ed. K. Werner & T. Rauch, 239

Wood, P. R. & Faulkner, D. J. 1986, *ApJ*, 307, 659



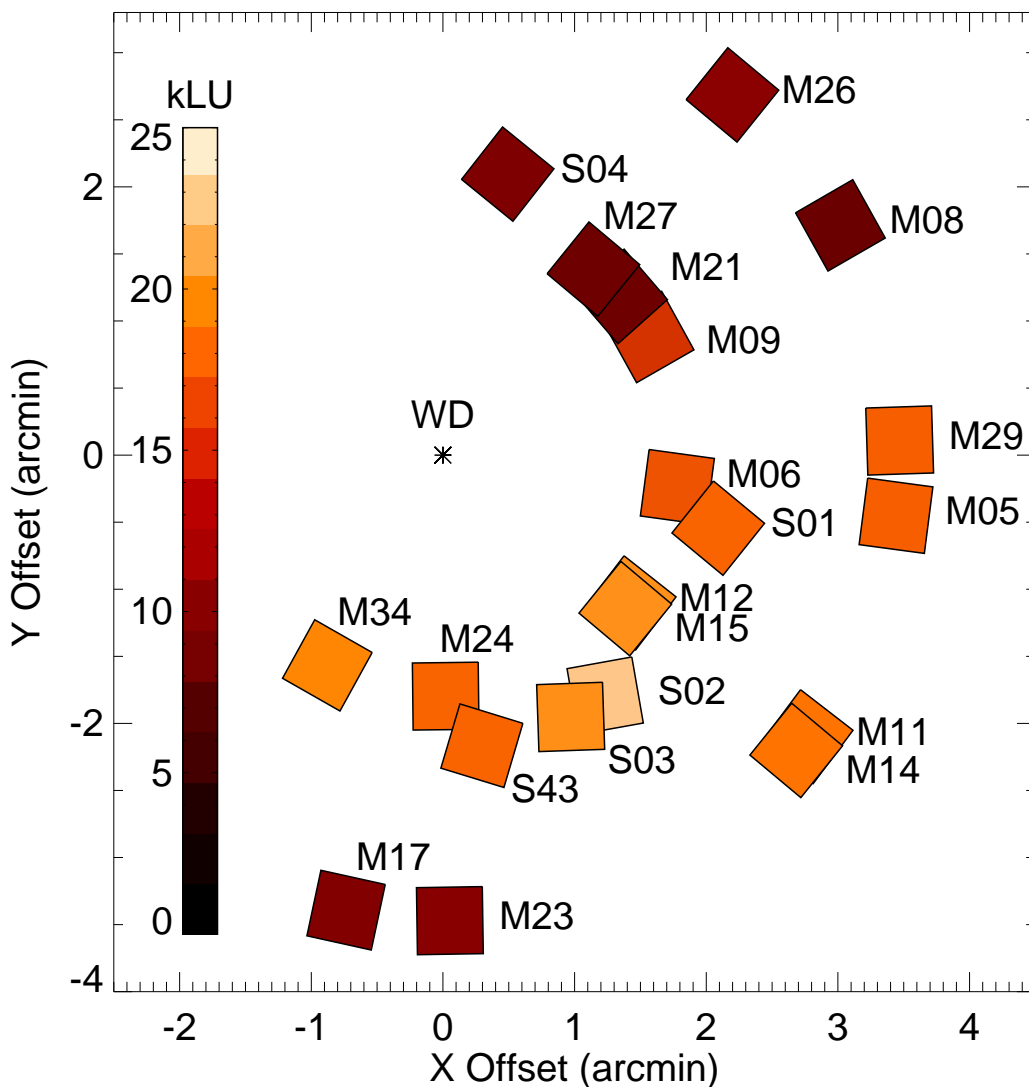


Fig. 1.— Observations of diffuse O VI emission around the hot white dwarf KPD 0005+5106. Colors represent the measured O VI  $\lambda 1032$  intensity in units of kLU ( $1 \text{ LU} = 1 \text{ photon s}^{-1} \text{ cm}^{-2} \text{ sr}^{-1}$ ) recorded through the *FUSE* LWRS aperture. For M17 and M26, the colors represent  $3\sigma$  upper limits. The radius of the outer ring is 3.5 arcmin. Labels refer to the map keys defined in Table 1. North is up and east is to the left.

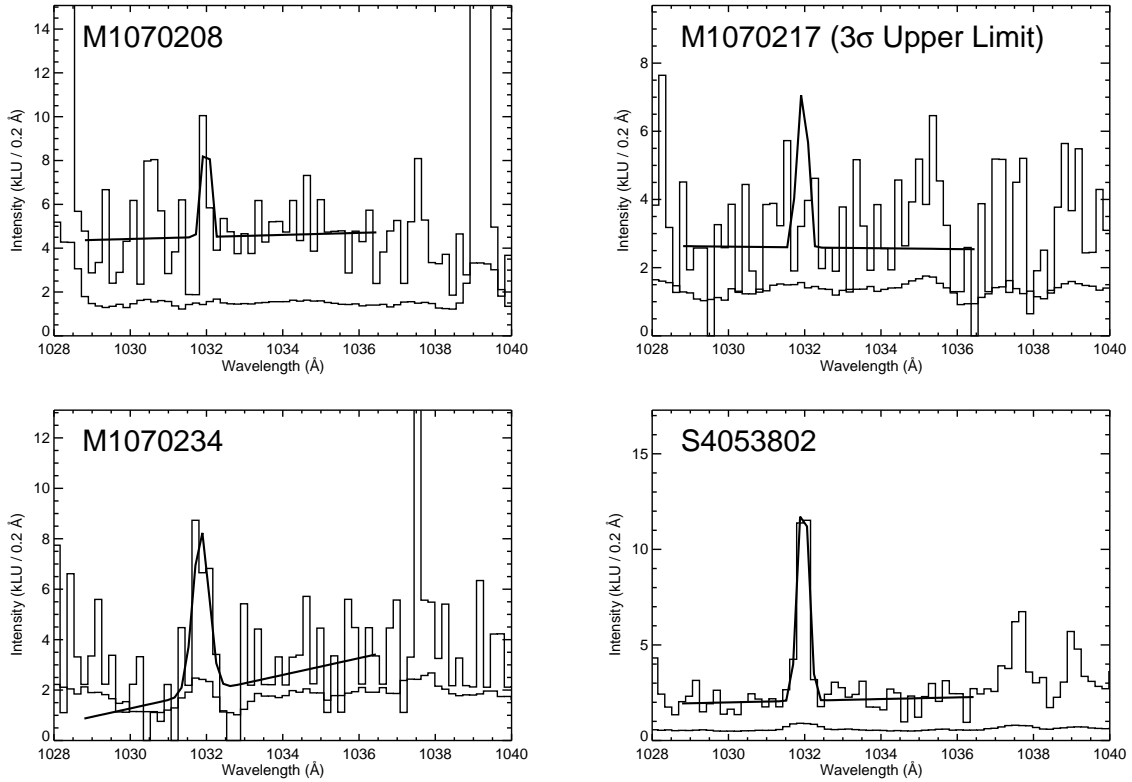


Fig. 2.— Selected spectra showing the region around O VI  $\lambda$ 1032. The data are binned by 14 pixels, and best-fit model and error spectra are overplotted. For M1070217, the model spectrum represents a  $3\sigma$  upper limit. Interstellar C II \*  $\lambda$ 1037 and O VI  $\lambda$ 1038 are present in some spectra, as are the geocoronal [O I]  $\lambda\lambda$ 1028, 1039 lines.

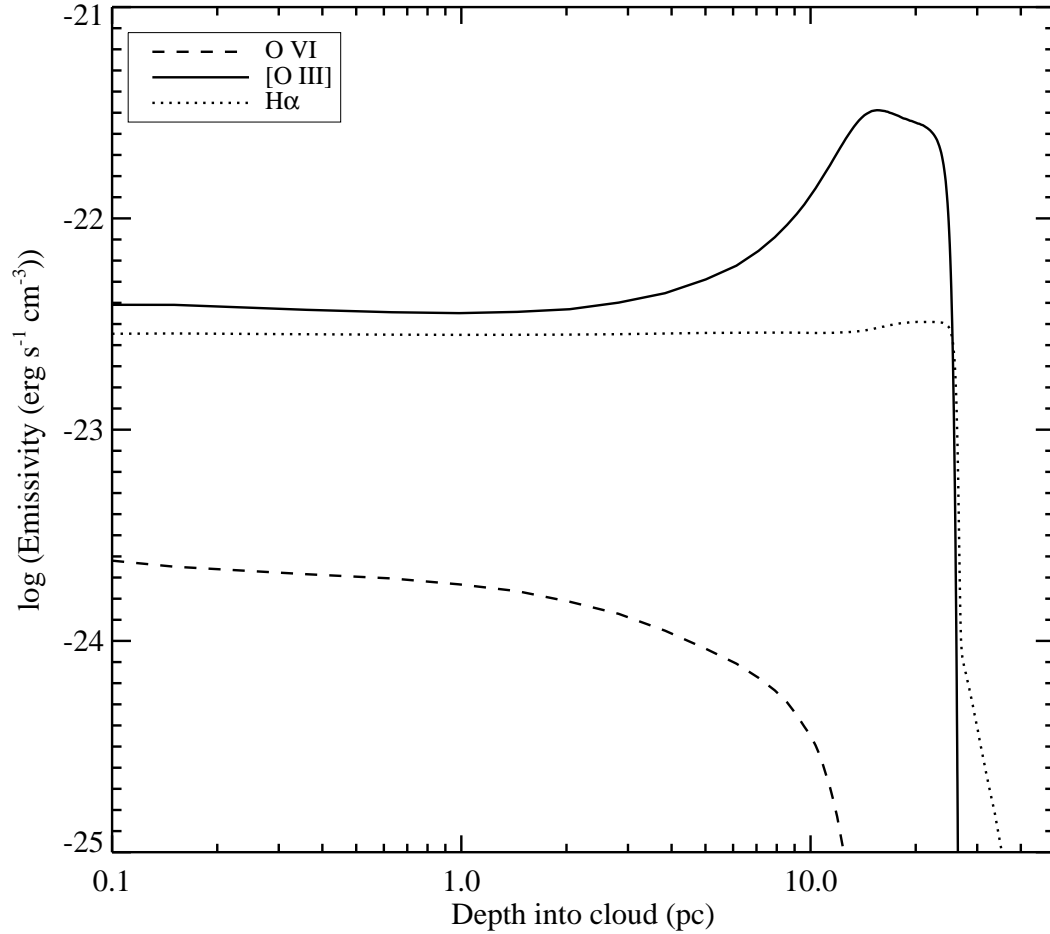


Fig. 3.— Emissivities of selected lines predicted by the fiducial model for the nebula. The O VI emissivity translates to an observed intensity of 17,300 LU, consistent with the *FUSE* data. The [O III] emission extends out to about 27 pc, consistent with optical observations.

Table 1. Observations

Observation ID	Date	Position Angle <sup>a</sup> (degrees)	Distance (arcmin)	Map Key
M1070205	2001 Sep 29	263	3.5	M05
M1070206	2001 Sep 29	262	1.8	M06
M1070208	2002 Sep 23	300	3.5	M08
M1070209	2002 Sep 23	299	1.8	M09
M1070211	2002 Oct 21	233	3.5	M11
M1070212	2002 Oct 22	232	1.8	M12
M1070214	2002 Oct 23	231	3.5	M14
M1070215	2002 Oct 23	230	1.8	M15
M1070217	2002 Dec 17	168	3.5	M17
M1070221	2003 Sep 07	311	1.8	M21
M1070223	2003 Dec 03	181	3.5	M23
M1070224	2003 Dec 03	181	1.8	M24
M1070226	2004 Jul 24	321	3.5	M26
M1070227	2004 Jul 24	321	1.8	M27
M1070229	2006 Sep 02	272	3.5	M29
M1070234	2006 Dec 26	151	1.8	M34
S4053801	2001 Oct 23	256	2.2	S01
S4053802	2004 Nov 23	215	2.2	S02
S4053803	2003 Dec 02	207	2.2	S03
S4053804	2004 Jul 23	346	2.2	S04
S4054403	2002 Dec 22	188	2.2	S43

<sup>a</sup>Position angle of LWRS aperture, measured east of north, relative to the star.

Table 2. Measured O VI Intensities and Upper Limits

Sight Line	Time <sup>a</sup> (s)	Intensity <sup>b</sup> (kLU)	S/N <sup>c</sup>	$v_{\text{LSR}}$ (km s <sup>-1</sup> )	FWHM <sup>d</sup> (km s <sup>-1</sup> )
M34	1836	18.8 ± 6.2	3.0	-13 ± 23	120 ± 60
S43/M24	6147	17.0 ± 2.5	6.9	4 ± 7	10 ± 30
S03	9596	19.3 ± 2.7	7.3	8 ± 7	50 ± 30
S02	14800	22.1 ± 2.0	11.1	18 ± 5	50 ± 20
M12/M15	8029	19.4 ± 2.8	7.0	11 ± 7	50 ± 40
S01	10703	17.0 ± 1.8	9.5	7 ± 5	7 ± 40
M06	3581	16.1 ± 3.8	4.2	13 ± 11	20 ± 80
M09	4330	14.5 ± 3.5	4.1	8 ± 16	120 ± 50
M21/M27	6048	7.6 ± 2.3	3.3	40 ± 14	10 ± 110
S04	4111	8.7 ± 2.2	4.0	4 ± 11	20 ± 110
M17	3160	< 9.0			
M23	2521	9.4 ± 3.0	3.1	8 ± 16	10 ± 140
M11/M14	6346	17.8 ± 2.5	7.2	8 ± 7	10 ± 30
M05/M29	4457	16.7 ± 2.8	5.9	4 ± 8	10 ± 100
M08	4214	7.3 ± 2.5	2.9	26 ± 9	3 ± 30
M26	2806	< 9.5			

<sup>a</sup>Total exposure time.

<sup>b</sup>1 LU = 1 photon s<sup>-1</sup> cm<sup>-2</sup> sr<sup>-1</sup>.

<sup>c</sup>Statistical significance of quoted intensity,  $I/\sigma(I)$ .

<sup>d</sup>Gaussian FWHM values include the smoothing imparted by the instrument optics. Values less than  $\sim 25$  km s<sup>-1</sup> indicate that the emission feature is unresolved.